Society For Biomaterials

Toxicity of graphene nanoflakes evaluated by cell-based electrochemical impedance biosensing

Ok Ja Yoon,[1*] Insu Kim,[1*] Il Yung Sohn,[1] Truong Thuy Kieu,[1] Nae-Eung Lee[1,2,3]

[1]School of Advanced Materials Science and Engineering and Center for Human Interface Nanotechnology, Sungkyunkwan University, Suwon, Kyunggi-do 440-746, Korea
[2]SKKU Advanced Institute of Nanotechnology (SAINT), Sungkyunkwan University, Suwon, Kyunggi-do 440-746, Korea
[3]Samsung Advanced Institute for Health Sciences and Technology (SAIHST), Sungkyunkwan University, Suwon, Kyunggi-do 440-746, Korea

Received 3 April 2013; revised 11 July 2013; accepted 17 July 2013
Published online 19 August 2013 in Wiley Online Library (wileyonlinelibrary.com). DOI: 10.1002/jbm.a.34886

Abstract: Graphene nanoflake toxicity was analyzed using cell-based electrochemical impedance biosensing with interdigitated indium tin oxide (ITO) electrodes installed in a custom-built mini- incubator positioned on an inverted optical microscope. Sensing with electrochemical measurements from interdigitated ITO electrodes was highly linear ($R^2 = 0.93$ and 0.96 for anodic peak current (I_{pa}) and cathodic peak current (I_{pc}), respectively). Size-dependent analysis of Graphene nanoflake toxicity was carried out in a mini-incubator system with cultured HeLa cells treated with Graphene nanoflakes having an average size of 80 or 30 nm for one day. Biological assays of cell proliferation and viability complemented electrochemical impedance measurements. The increased toxicity of smaller Graphene nanoflakes (30 nm) as measured by electrochemical impedance sensing and optical monitoring of treated cells was consistent with the biological assay results. Cell-based electrochemical impedance biosensing can be used to assess the toxicity of nanomaterials with different biomedical and environmental applications. © 2013 Wiley Periodicals, Inc. J Biomed Mater Res Part A: 102A: 2288–2294, 2014.

Key Words: graphene, electrochemical impedance biosensor, ITO electrode, HeLa cells, toxicity analysis

How to cite this article: Yoon OJ, Kim I, Sohn IY, Kieu TT, Lee N-E. 2014. Toxicity of graphene nanoflakes evaluated by cell-based electrochemical impedance biosensing. J Biomed Mater Res Part A 2014:102A:2288–2294.

INTRODUCTION

Recently, two-dimensional carbon nanomaterials, such as graphene, have shown some toxic[1] and safety effects in biomedical applications, such as tissue engineering,[2] bioimaging,[3] drug delivery,[4, 5] and photo thermal cancer therapy.[6] The main parameters affecting cytotoxicity nanomaterials, including graphene,[7] graphene oxide (GO),[8] carbon nanotubes (CNTs),[9,10] and gold and silver nanoparticles[11] *in vivo* and *in vitro* are concentration, shape, size, and surface state. In general, previous research has reported that graphene has a relatively low toxicity compared to CNT in biological assays.[12] GO is considered more biocompatible than graphene because it resulted in less damage and toxicity in human skin fibroblasts, red blood cells, and bacteria due to higher surface oxygen content, larger surface charges, and good dispersion.[13,14]

Biological assays of cell activity and viability evaluation, such as measuring the mitochondrial reduction of tetrazolium salts into an insoluble dye (the MTT test), the release of the enzyme lactate dehydrogenase (LDH), and the measurement of reactive oxygen species (ROS), are often used to evaluate toxicity.[15] These methods are complex, costly, and difficult for long-term monitoring of cells. In contrast, electrochemical sensing to assess toxicity has shown low cost, high sensitivity, good selectivity, fast response, small size, capability of long-term monitoring or real-time measurements, and reproducible results.[16] In particular, electrochemical sensors are promising tools to detect toxic chemical compounds in industrial products, environmental samples, or biological systems *in vivo* and *in vitro*.[17] Electric cell-substrate impedance sensing (ECIS) has been used to analyze toxicity by detecting changes in resistance caused by cells attaching to and spreading on the electrode surface, morphological change of cells, and micromotion in the cell culture.[18]

Recently, toxicity analysis to investigate the effects of GO nanoflake concentration and size was reported *in vitro* and *in vivo* through various biological assays, including for ROS generation, LDH release, and apoptosis.[8] However, the toxicity of

Additional Supporting Information may be found in the online version of this article.
*These authors contributed equally to this work.
Correspondence to: Nae-Eung Lee; e-mail: nelee@skku.edu
Contract grant sponsor: Basic Science Research Program; contract grant numbers: 2009-0083540, 2012R1A1A3008822
Contract grant sponsor: WCU Program; contract grant number: R32-2008-000-10124-0
Contract grant sponsor: Ministry of Education, Science and Technology (MEST), Korea: contract grant number: NRF-2011-355-D00098

size-controlled graphene nanoflakes analyzed using cell-based electrochemical impedance biosensor, optical monitoring of cells, and biological assays has not been reported yet.

We investigated the following:

1. The fabrication of an electrochemical impedance biosensor with interdigitated transparent indium tin oxide (ITO) electrodes on glass.
2. The integration of cell-based electrochemical impedance biosensor into a custom-built mini-incubator positioned on the stage of an inverted optical microscope.
3. The ability of impedance monitored in the custom-built mini-incubator to analyze the toxicity of size-controlled graphene nanoflakes using HeLa cells treated for one day.

The ITO interdigitated electrodes for ECIS were designed as working and counter electrodes by photolithography to allow for good linearity, transparency, and a large active area. We analyzed the toxicity of graphene nanoflakes having an average size of 80.9 ± 5.5 and 30.9 ± 5.4 nm at the same concentration (400 μg/mL). Biological assays were used to complement the toxicity analysis by ECIS. These results proved applicability of EICS to measure the toxicity of nanomaterials.

MATERIALS AND METHODS

Preparation of graphene nanoflakes

GO nanoflakes were synthesized from purified natural graphite flakes (purchased from Sigma Aldrich) by a modified Hummers method.[19] The GO nanoflakes (6 mg) mixed with deionized water (2 mL), followed by ultrasonication for 2 hr. The solution was then mixed with *N, N'*-dimethylformamide (99.5%, Junsei, Tokyo, Japan) solvent (15 mL) and hydrazine hydrate solution (24–26%, Sigma Aldrich; 1 mL). The mixture was stirred for 24 hr at 80°C to reduce GO. The mixture was washed with ethanol at room temperature.

Fabrication and characterization of the interdigitated ITO electrode

ITO electrodes were used as working and counter electrodes and a Pt wire was used as the reference electrode. To fabricate ITO electrodes, ITO glass substrates were purchased from Fine Chemicals (Korea). ITO has are resistivity of < 20 ohmsq^{-1}, thickness of 80 nm, and transmittance of 87%. The counter and working electrodes were fabricated on an ITO-coated glass substrate by wet etching in 24 wt % HCl followed by a photolithography process.

The fabricated ITO electrodes were characterized by cyclic voltammetry (CV) in 10 mM $K_3[Fe(CN)_6]$ using a potentiostat electrochemical workstation (Bio-Logic Science Instruments, VSP, France). The CV measurements were carried out at a potential range of -0.5 to 0.5 V versus a Pt wire with scan rates of 15, 25, 35, 45, 55, 65, 75, 85, 95, 100, 150, and 200 mVs^{-1}.

Glass substrates with fabricated ITO electrodes were positioned at the bottom of two culture wells in a custom-built mini-incubator. The Pt wire was fixed to the cover of the culture well as a reference electrode. The volume of the culture wells inside the mini-incubator was 700 μL.

Cell culture

HeLa cells were purchased from the Korea Cell Line Bank (Seoul, Korea). These cells were cultured in Rose well Park Memorial Institute (RPMI) supplemented with 10% heat-inactivated fetal bovine serum (FBS) along with a 1% antibiotic mixture (Invitrogen) in a 95% humidified air and 5% CO_2 atmosphere at 37°C. After reaching about 80% confluency, cells were subcultured by trypsinization. Cells were plated in 600 μL containing $\sim 10^6$ cells per well for 1 day and grown for 1 day after adding size-controlled graphene nanoflakes (100 μL of a 400 μg/mL solution) in the custom-built mini-incubator integrated with the cell-based electrochemical impedance biosensor. The schematic of EICS integrated into the mini-incubator is shown in the Figure 1(a). The mini-incubator integrated with the ITO impedance sensor electrodes was placed on the stage of an inverted optical microscope (AE30/31, Motic Incorporation) to obtain the optical images of cells during ECIS measurements.

Electrochemical cytotoxicity analysis

To disperse graphene nanoflakes in RPMI, 5 mL of medium was mixed with 2 mg of graphene nanoflakes having an average size of 80.9 ± 5.5 or 30.9 ± 5.4 nm (400 μg/mL). The solutions were dispersed for 24–72 hr using sonication. HeLa cells toxicity was measured every 6 hr for 1 day after adding the graphene solution (100 μL) using the mini-cell incubator system integrated with electrochemical impedance sensor containing custom-built mini-incubator. The impedance of control cells (untreated) and cells treated with graphene solutions was measured using the potentiostat electrochemical workstation. Impedance was measured with a potential sweep range from -10 to 10 V at a frequency range of 10 kHz–100 MHz versus a Pt reference electrode.

Biological assays of cell proliferation and viability

Cell proliferation was quantified using a WST-1 assay (Takara Biomedical) by measuring the metabolic activities of viable cells. Briefly, HeLa cells were plated and cultured in the custom-built mini-incubator integrated with the electrochemical sensor. Then, these cells were mixed with WST-1 solution (0.1 mL) in 1 mL of growth medium and incubated for 3 hr at 37°C with 5% CO_2 in a humidified atmosphere. A 110-μL aliquot was transferred to a 96-well plate, and the absorbance was measured with a microplate reader (Bio-Rad) at 440 nm. The absorbance at 690 nm was measured separately using a spectrophotometer (SpectraMax M5, Molecular Devices) as a reference. Each experiment was performed in triplicate, and the measured data are shown with standard deviations. Student's t-test was used to analyze the relationships between variables. A p value < 0.05 was considered statistically significant.

Analytical methods

The thicknesses of the graphene nanoflakes were analyzed by high-resolution transmission electron microscopy

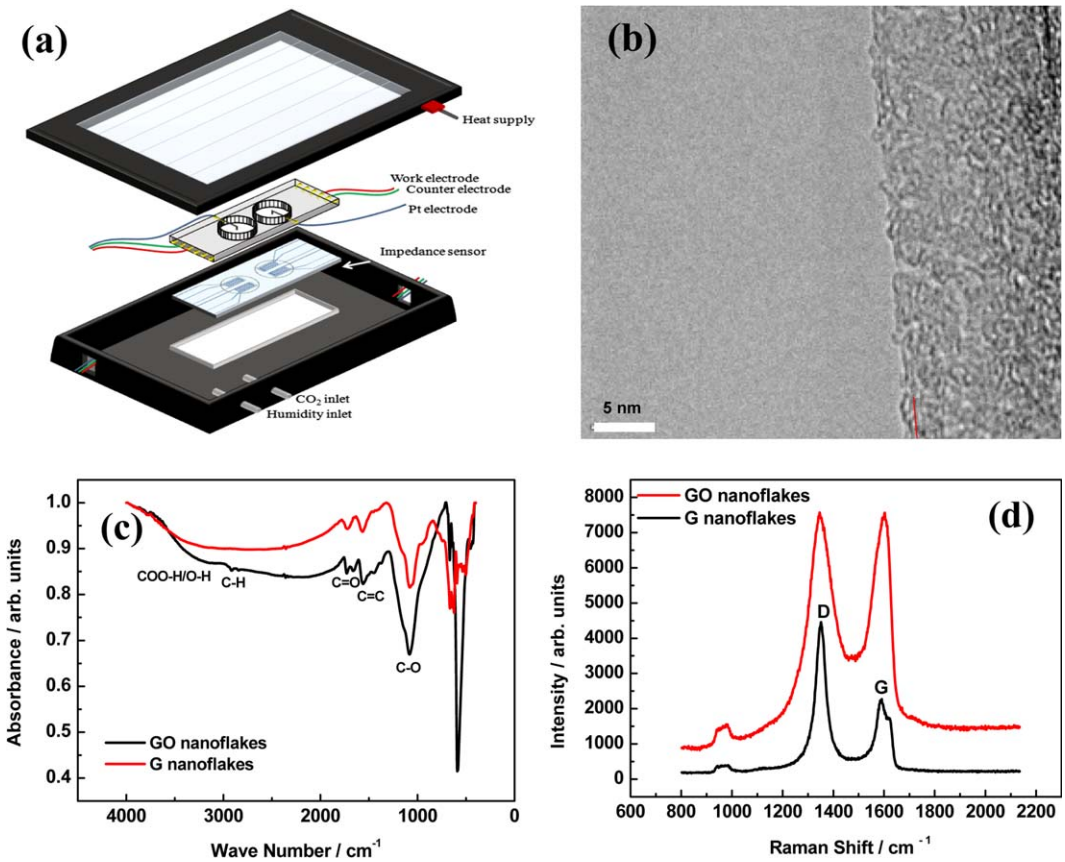

FIGURE 1. (a) The schematics diagram of the mini-incubator integrated with the impedance sensor electrodes. (b) The HR-TEM image and thickness of graphene described the line, (c) FT-IR spectra of GO and graphene nanoflakes, and (d) Micro-Raman spectra of GO and graphene nanoflakes. [Color figure can be viewed in the online issue, which is available at wileyonlinelibrary.com.]

(HR-TEM) (JEW 2100F, JEOL). The morphology and size of graphene nanoflakes was measured using field-emission scanning electron microscopy (FE-SEM) (JSM 890, JEOL) at gentle beam mode at an acceleration of 10 keV to avoid electron beam induced damage. Micro-Raman spectra of graphene nanoflakes were obtained under ambient conditions using the 514.5-nm line of an argon ion laser. Raman measurements were performed using backscattering geometry with a JY LabRam HR fit with a liquid-nitrogen cooled CCD detector. The graphene nanoflake surfaces were characterized by Fourier-transform infrared spectroscopy (FT-IR) (Bruker IFS-66/S, Bruker Corporation). The interdigitated electrode of a cell-based electrochemical sensor was imaged using an inverted microscope (Olympus Corporation, IX 81) and FE-SEM (JSM 890, JEOL).

RESULTS AND DISCUSSION

Characteristics of graphene nanoflakes

Typical FE-SEM images of graphene nanoflakes show average sizes of 80.9 ± 5.5 and 30.9 ± 5.4 nm when sonicated for 24 and 72 hr in water as shown in Supporting Information Figures S1(a, b), respectively. The average thickness of the graphene, measured by HR-TEM, was less than 1.2 nm in Figure 1(b). The FE-SEM images in Supporting Information Figures S1(a, b) also shows that graphene nanoflakes are well dispersed in water. Figure 1(c) shows the FT-IR spectra (4,500–500 cm^{-1}) of the GO and graphene nanoflakes. The absorption intensity distributions due to stretching and vibration of oxygen groups, such as COO—H/O—H, and C—H disappeared from the graphene nanoflakes as a result of reduced GO. The intensity of C═O, C═C, and C—O stretching and vibration also decreased.[20] Micro-Raman spectra were obtained for GO and graphene nanoflakes to investigate changes in their chemical bond configurations after forming graphene nanoflakes [Fig. 1(d)]. The Raman peaks of GO nanoflakes were located at about 1357 and 1599 cm^{-1} with a graphene-band to D-band intensity ratio (I_D/I_G) of 1.06. Shifts in the graphene-band from the Raman spectra from graphene nanoflakes indicate that the oxygen-containing functional groups on GO nanoflakes have been reduced.[21] The disorder-induced D mode and C—C stretching graphene mode of graphene nanoflakes were located at about 1352 and 1594 cm^{-1}, respectively, and the I_D/I_G increased to1.33 after reduction. Our data show that the I_D/I_G in graphene nanoflakes was significantly higher than in GO nanoflakes. The increased D mode intensity of graphene nanoflakes was caused by defects induced by the hydrazine vapor treatment.

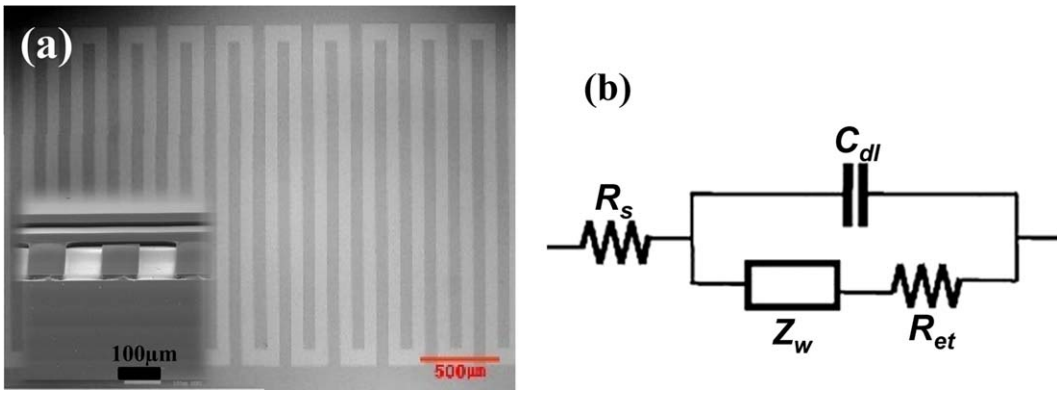

FIGURE 2. (a) FE-SEM image of patterned, interdigitated working, and counter ITO electrodes. The inset shows the cross-section of the patterned ITO electrode. (b) Randle equivalent circuit model for the impedance analysis. [Color figure can be viewed in the online issue, which is available at wileyonlinelibrary.com.]

Electrochemical characterizations of interdigitated ITO electrodes

The impedance biosensor is equipped with working and counter ITO electrodes and a Pt reference electrode. The working and counter electrodes were designed as an interdigitated electrode to increase linearity, transparency, and the active area, as shown in Figure 2(a). The counter and working electrodes each had an electrode area of 0.047 cm^2 and were fabricated on an ITO-coated glass substrate. A cross-section FE-SEM image of the patterned ITO electrodes is shown as an inset in Figure 2(a).

To characterize the interdigitated electrodes, CV data of an interdigitated ITO electrode versus Pt at different scan rates, v (15, 25, 35, 45, 55, 65, 75, 85, 95, 100, 150, and 200 mVs^{-1}) in 10 mM $K_3[Fe(CN)_6]$ were obtained and are shown Supporting Information Figures S1(c). The anodic peak currents (I_{pa}) shifted to the right as v increased in the reversible redox system. The relationships of the cathodic peak currents (I_{pc}) and anodic peak currents (I_{pa}) with v are shown in Supporting Information Figures S1(d). The linear regression equations of I_{pa} and I_{pc} are given by $I_{pa} = 2.50 \times 10^{-4}\ v + 0.019$ (mA, mVs^{-1}, $R^2 = 0.93$) and $I_{pc} = -2.12 \times 10^{-4}\ v - 0.013$ (mA, mVs^{-1}, $R^2 = 0.96$), with $I_{pa}/I_{pc} = 1.1$, indicating a reversible process (I_{pa}/I_{pc} is close to 1).[22] The fabricated interdigitated electrodes were highly linear (R^2 values of I_{pa} and I_{pc} are 0.93 and 0.96, respectively) in a small sample volume (700 μL) indicating of excellent electrochemical behavior.

Cell-based electrochemical impedance measurements to analyze graphene nanoflakes toxicity

To analyze the toxicity of graphene nanoflakes of different sizes (80 and 30 nm), impedance was monitored for 1 day after treating cells with two graphene solutions. Cells were plated with a density of $\sim 10^6$ per well, treated with graphene nanoflakes, and incubated for 1 day in a 95% humidified air, 5% CO_2 atmosphere, and at 37°C. One culture well was not treated as a control. Impedance changes due to cell proliferation on the electrode surface were measured three times after the treatments (Fig. 3). ECIS results were analyzed by Randle's circuit model assuming the model was equivalent to electrochemical interface processes that depend on the physic-chemical parameters of Z_w (Warburg impedance of semi-infinite diffusion mechanism), C_{dl} (the double layer capacitance), R_{et} (the electron transfer resistance of redox couple), and R_s (the solution resistance of the modified working electrode and the Pt reference electrode).[23] The equivalence scheme for Randle's circuit model and ECIS is shown in Figure 2(b).

Typical impedance results are presented in Nyquist diagrams (Fig. 3) as plots of the imaginary component impedance (Z'') versus the real component impedance (Z') at a frequency range of 100 kHz. Here, the batches for the cells in Figures 3(a, b) and Figure 3(c, d) were the same. The R_{et} data were obtained from the Nyquist plots acquired from the three batches of cultured cells [see the insets in Fig. 3(a–d)] and the mean standard deviation was indicated as error bar. The Nyquist diagrams obtained from untreated control cells in Figure 3(a,c) indicated nontoxicity by increased R_{et}, determined by the interface properties of the electrode surface [see the insets in Fig. 3(a,c)]. Cells attached to the electrode were electron-transfer resistant.[24] The impedance values for control cells in Figures 3(a,c) were different because the number of cells and culture conditions were not identical. The Nyquist diagram in Figure 3(b) for HeLa cells treated with 80-nm graphene nanoflakes showed nontoxicity, as indicated by the increased R_{et} values in the insets of Figures 3(b) similarly to the R_{et} values in the insets of Figures 3(a,c). The Nyquist diagram in Figure 3(d) for cells treated with 30-nm graphene nanoflakes, however, indicates toxicity, as shown by decreased R_{et} values implying decreased HeLa cell proliferation [the inset in Fig. 3(d)]. Decreased R_{et} values in Figure 3(d) indicate HeLa cell apoptosis caused by toxicity of graphene nanoflakes. Decreasing resistance from cells treated with 30-nm graphene nanoflakes compared to increasing resistance from cells treated with 80-nm graphene nanoflakes confirmed increased toxicity in cells treated with smaller graphene nanoflakes. Our results prove that cells treated with smaller nanostructures had an increased R_{et} value in impedance

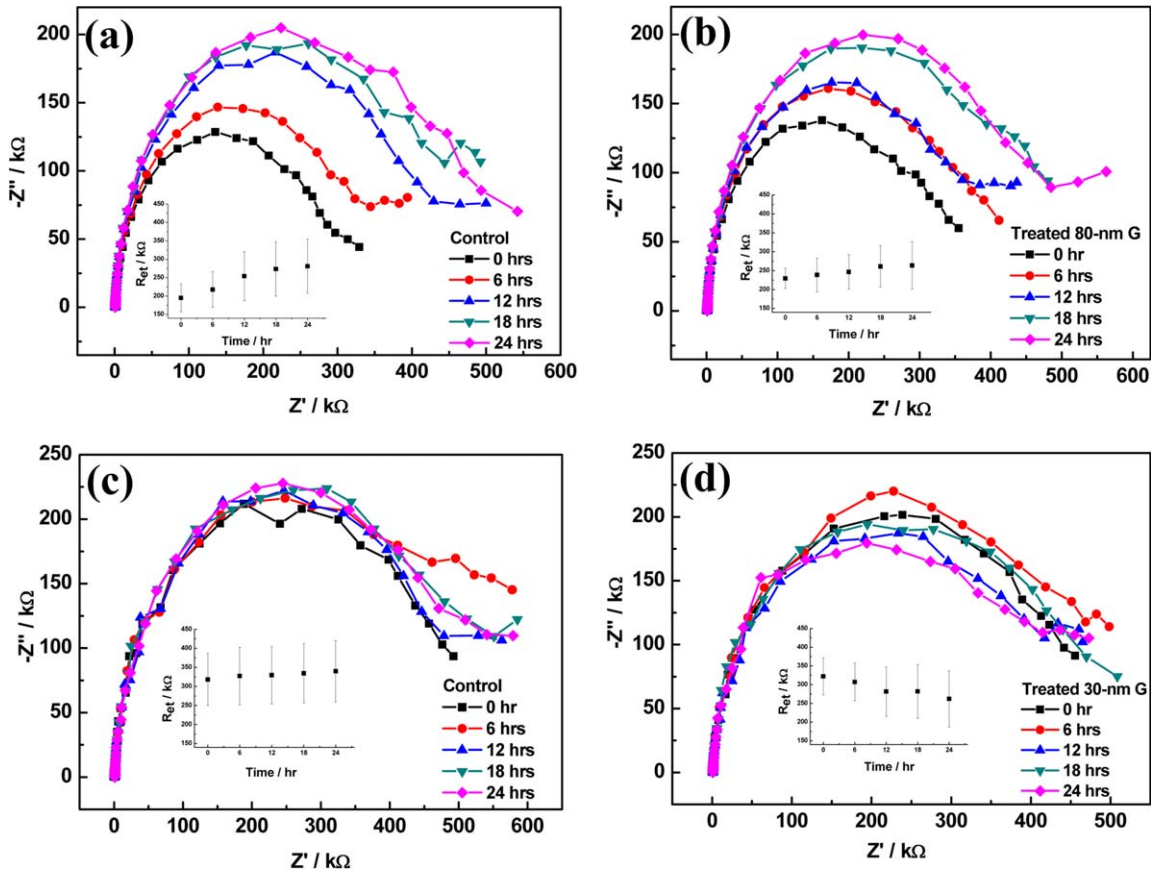

FIGURE 3. Nyquist diagrams obtained from (a) and (c) untreated cells, (b) cells treated with 80-nm graphene nanoflakes, and (d) cells treated with 30-nm graphene nanoflakes. The error bars indicate the mean standard deviation of the R_{et} values obtained from three batches of cultured cells. [Color figure can be viewed in the online issue, which is available at wileyonlinelibrary.com.]

analysis. Similar to a previous report, evaluating the toxicity of nanomaterials with different sizes indicates the importance of nanomaterial size in biocompatibility.[8]

The optical images in Figure 4(a–c) show HeLa cell morphology on the electrode surface after 1 day of biosensing and the additional optical images of the monitored cells every 6 hr for 1 day were also shown in the Supporting Information Figure S2(a,b). The optical monitoring of the cells as times goes by after treated with graphene nanoflakes confirmed increasing cell death, damage, and detachment by apoptosis compared with the control cells, in consistent with the results of ECIS. Control HeLa cells [Fig. 4(a)] appeared healthy due to cell proliferation and viability. Images of cells treated with 80-nm graphene nanoflakes [Fig. 4(b)] confirmed the aggregation of graphene nanoflakes, presumably due to their hydrophobic properties, in contrast to no segregation of 30-nm graphene nanoflakes [Fig. 4(c)]. Nanostructured materials such as hydrophobic pristine graphene accumulating on plasma membranes of HeLa cells were reported to generate high oxidative stress, causing toxicity and apoptosis.[25] In this work, however, the smaller 30-nm graphene nanoflakes which did not aggregate on cell membranes induced apoptosis due to higher uptake by cells while the 80-nm graphene nanoflakes agglomerated on cell membranes caused less toxicity. Stabilized small-size nanostructured materials proved outstanding in cellular uptakes.[26] Therefore, the size of nanostructured materials is a critical parameter affecting their toxicity.

Similar to the observed dependence of toxicity on graphene nanoflake size in the present experiment, GO or graphene size has been reported to affect toxicity.[27] Larger GO and graphene nanoflakes are more biocompatible.[8,27] Recently, there has been research on GO or graphene nanoflakes for various biological applications. For example, GO nanoflakes less than 50 or 100 nm were reported to enter cells with cargos, such as molecular beacon and polyethylene glycol for DNA/drug delivery.[4,28] A multifunctionalized GO, smaller than 200 nm, with folic acid conjugated Fe_3O_4 nanoparticles was used for dual-targeted drug delivery.[5] 2D PEGylated nano-graphene smaller than10 nm was used to passively target tumors.[29] Because the size of graphene nanoflakes is expected to affect cytotoxicity as well as endocytosis and cellular uptake, the toxicity of graphene nanomaterials for biomedical applications should be studied in more detail.

Analysis of cell viability by bioassay measurements

To evaluate graphene nanoflake toxicity, the proliferation and viability of HeLa cells treated for 1 day with graphene nanoflakes in mini-incubator with the cell-based electrochemical

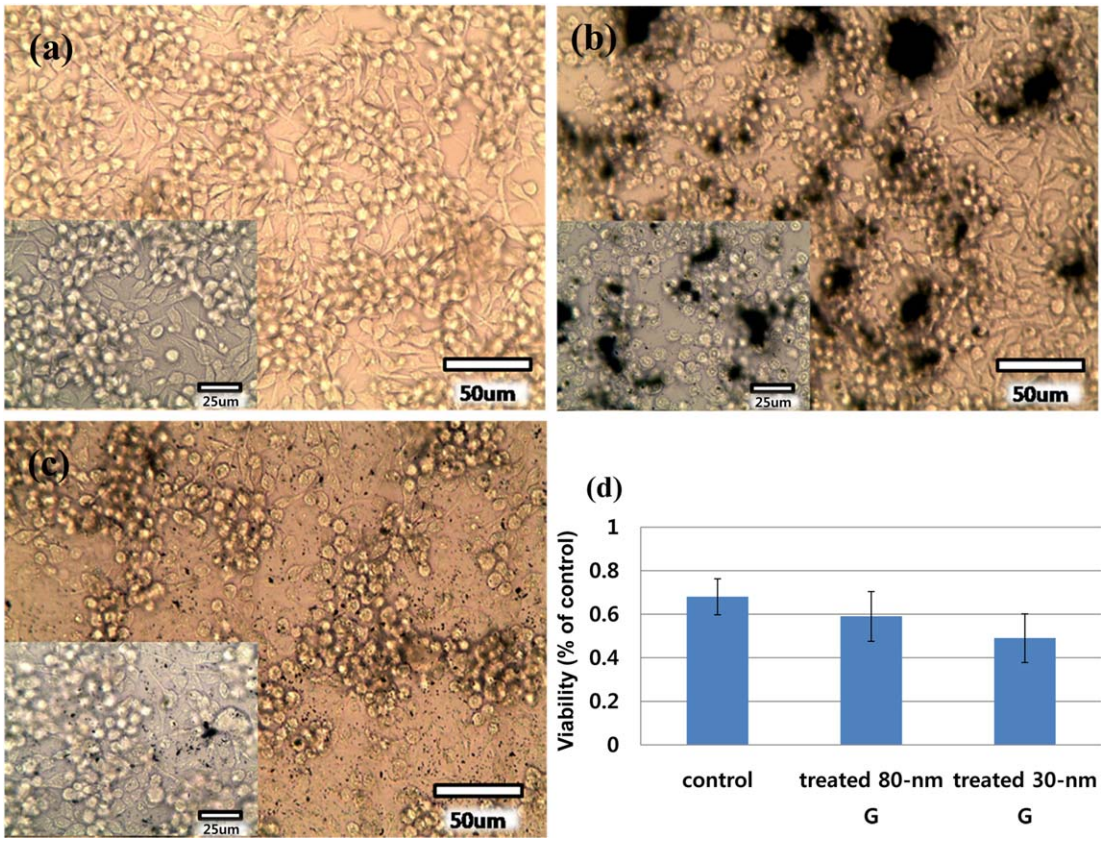

FIGURE 4. Images of (a) control HeLa cells, (b) HeLa cells treated with 80-nm graphene nanoflakes, and (c) HeLa cells treated with 30-nm graphene nanoflakes. (magnification of the images, ×200 and magnification of the inserted images, ×400) (d) proliferation and viability of cells assessed through a WST-1 assay ($n = 3$, $p < 0.05$). [Color figure can be viewed in the online issue, which is available at wileyonlinelibrary.com.]

impedance sensor were measured through a biological WST-1assay. The WST-1 assay results for three batches of measurements are presented as mean ± standard deviation and considered significant by Student's t-test with p values of < 0.05. One culture well in the mini-incubator remained untreated as a control. The WST-1 assay results of Figure 4(d) demonstrates a prominent decrease in metabolic activity for cells treated with 30- and 80-nm graphene nanoflakes compared to control cells. Proliferation and viability of cells treated with 80-nm graphene nanoflakes was apparent slightly lower than control cells but higher than those of cells treated with 30-nm graphene nanoflakes at the same concentration. These results show that toxicity results as measured by electrochemical impedance were consistent with toxicity results obtained by the biological assay. Analyzing toxicity by cell-based electrochemical impedance is important for assessing the toxicity of nanomaterials with biomedical, drug, or environmental applications.

CONCLUSIONS

A cell-based electrochemical impedance sensor based on interdigitated ITO electrodes was prepared to evaluate size-dependent toxicity of graphene nanoflakes. Interdigitated electrodes were integrated into culture wells in a custom-built mini-incubator and had good electrochemical characteristics. Size-dependent toxicity of graphene nanoflakes was analyzed using impedance sensing and optical images of cells of HeLa cells cultured in the mini-incubator for 1 day after treatment with 80, 30-nm graphene nanoflakes of different sizes. Our studies consistently showed increased toxicity with smaller graphene nanoflakes for electrochemical impedance sensing, optical images of cells, and also bioassays. These results demonstrate the importance of size-dependent graphene nanoflake toxicity in biological systems. The method can be effectively applied to assess the toxicity of nanomaterials, drugs, and environmental toxins.

REFERENCES

1. Singh V, Joung D, Zhai L, Das S, Khondaker S, Seal S. Graphene based materials: Past, present and future. Prog Mater Sci 2011;56: 1178–1271.
2. Depan D, Girase B, Shah JS, Misra RDK. Structure-process-property relationship of polar graphene oxide mediated cellular response and stimulated growth of osteoblasts. Acta Biomater 2011;7:3432–3445.
3. Wang H, Zhang Q, Chu X, Chen T, Ge J, Yu R. Graphene oxide–peptide conjugate as an intracellular protease sensor for caspase-3 activation imaging in live cells. Angew Chem Int Ed Engl 2011; 50:7065–7069.
4. Liu Z, Robinson JT, Sun X, Dai H. PEGylated nanographene oxide for delivery of water-insoluble cancer drugs. J Am Chem Soc 2008;130:10876–10877.
5. Yang XY, Wang YS, Huang X, Ma YF, Huang Y, Yang YG, Duana RHQ, Chen YS. Multi-functionalized graphene oxide based

anticancer drug-carrier with dual-targeting function and pH-sensitivity. J Mater Chem 2011;21:3448–3454.
6. Markovic ZM, Harhaji-Trajkovic LM, Todorovic-Markovic BM, Kepic DP, Arsikin KM, Jovanovic SP, Pantovic AC, Dramicanin MD, Trajkovic VS. In vitro comparison of the photothermal anticancer activity of graphene nanoparticles and carbon nanotubes. Biomaterials 2011;32:1121–1129.
7. Hu W, Peng C, Luo W, Lv M, Li X, Li D, Huang Q, Fan C, Graphene-based antibacterial paper. ASC Nano 2010;4:4317–4323.
8. Chang Y, Yang S-T, Liu J-H, Dong E, Wang Y, Cao A, Liu Y, Wang H. In vitro toxicity evaluation of graphene oxide on A549 cells. Toxicol Lett 2011;200:201–210.
9. Lam CW, James JT, McCluskey R, Arepalli S, Hunter RL. A review of carbon nanotube toxicity and assessment of potential occupational and environmental health risks. Crit Rev Toxicol 2006;36: 189–217.
10. Lee HJ, Park J, Yoon OJ, Kim HW, Lee DY, Kim DH, Lee WB, Lee N-E, Bonventre JV, Kim SS. Amine-modified single-walled carbon nanotubes protect neurons from injury in a rat stroke model. Nat Nanotechnol 2011;6:121–125.
11. Yen H-J, Hsu S-H, Tsai C-L. Cytotoxicity and immunological response of gold and silver nanoparticles of different sizes. Small 2009;5:1553–1561.
12. Zhang Y, Ali SF, Dervishi E, Xu Y, Li Z, Casciano D, Biris AS. Cytotoxicity effects of graphene and single-wall carbon nanotubes in neural phaeochromocytoma-derived PC12 cells. ACS Nano 2010; 4:3181–3186.
13. Akhavan O, Ghaderi E. Toxicity of graphene and graphene oxide nanowalls against bacteria. ACS Nano 2010;4:5731–5736.
14. Liao K-H, Lin Y-S, Macosko CW, Haynes CL. Cytotoxicity of graphene oxide and graphene in human erythrocytes and skin fibroblasts. ACS Appl Mater Interfaces 2010;3:2607–2615.
15. Thannickal VJ, Fanburg BL. Reactive oxygen species in cell signaling. Am J Physiol Lung Cell Mol Physiol 2000;279:L1005–L1028.
16. Rahman MM. Fabrication of L-lactate biosensor based on redox species mediated lactate oxidase using micro-device. Int J Biol Med Res 2010;1:9–14.
17. Hondroulis E, Liu C, Li C-Z. Whole cell based electrical impedance sensing approach for a rapid nanotoxicity assay. Nanotechnology 2010;21:1–9.
18. Male KB, Crowley SM, Collins SG, Tzeng Y-M, Luong JHT. Cell-based impedance spectroscopy for probing inhibitory effects of steroids and ergostane/lanosta-related compounds. Anal Methods 2010;2:870–877.
19. Yoon OJ, Jung CY, Sohn IY, Kim HJ, Hong B, Jhon MS, Lee N-E. Nanocomposite nanofibers of poly(d, l-lactic-co-glycolic acid) and graphene oxide nanosheets. Compos A 2011;42:1978–1984.
20. Shou QL, Cheng JP, Zhang L, Nelson BJ, and Zhang XB. Synthesis and characterization of a nanocomposite of goethite nanorods and reduced graphene oxide for electrochemical capacitors. J Solid State Chem 2012;185:191–197.
21. Jin M, Jeong H-K, Kim T-H, So KP, Cui Y, Yu WJ, Ra EJ, Lee YH. Synthesis and systematic characterization of functionalized graphene sheets generated by thermal exfoliation at low temperature. J Phys D: Appl Phys 2010;43:1–7.
22. Yin H, Ai S, Shi W, Zhu L. A novel hydrogen peroxide biosensor based on horseradish peroxidase immobilized on gold nanoparticles–silk fibroin modified glassy carbon electrode and direct electrochemistry of horseradish peroxidase. Sens Actuators B 2009;137:747–753.
23. Varshney M, Li Y. Interdigitated array microelectrodes based impedance biosensors for detection of bacterial cells. Review Biosens Bioelectron 2009;24:2951–2960.
24. Gu MM, Zhang JJ, Li Y, Jiang LP, Zhu JJ. Fabrication of a novel impedance cell sensor based on the polystyrene/polyaniline/Au nanocomposite. Talanta 2009;80:246–249.
25. Sasidharan A, Panchakarla LS, Chandran P, Menon D, Nair S, Rao CNR, Koyakutty M. Differential nano-bio interactions and toxicity effects of pristine *versus* functionalized graphene. Naoscale 2011; 3:2461–2462.
26. Hong BJ, Compton OC, An Z, Eryzazici I, Nguyen ST, Successful stabilization of graphene oxide in electrolyte solutions: Enhancement of bio-functionalization and cellular uptake. ACS Nano 2012; 6:63–73.
27. Akhavan O, Ghaderi E, Akhavan. Size-dependent genotoxicity of graphene nanoplatelets in human stem cells. Biomaterials 2012; 33:8017–8025.
28. Lu C-H, Zhu C-L, Li J, Liu J-J, Chen X, Yang H-H. Using graphene to protect DNA from cleavage during cellular delivery. Chem Commun 2010;46:3116–3118.
29. Yang K, Zhang SA, Zhang GX, Sun XM, Lee ST, Liu ZA. Graphene in mice: Ultrahigh in vivo tumor uptake and efficient photothermal therapy. Nano Lett 2010;10:3318–3323.
30. Sun XM, Liu Z, Welsher K, Robinson JT, Goodwin A, Zaric S, Dai H. Nano-graphene oxide for cellular imaging and drug delivery. Nano Res 2008;1:203–212.